Observation of the $t\bar{t}H$ production

Johannes Mellenthin, on behalf of the ATLAS Collaboration

II. Physikalisches Institut, Georg-August-Universität Göttingen, Friedrich-Hund-Platz 1, D-37077 Göttingen, Germany

E-mail: johannes.mellenthin@cern.ch

Abstract. The top quark is the heaviest elementary particle in the Standard Model, and has an expected Yukawa coupling of order unity. The value of this coupling is a key ingredient to unravel the nature of the observed Higgs boson. The most favourable production mode which has a direct sensitivity to this coupling is the production of a Higgs boson in association with a top-quark pair, $t\bar{t}H$. The observation of this process, based on the analysis of proton-proton collision data at a centre-of-mass energy of 13 TeV with the ATLAS detector at the Large Hadron Collider, is presented.

1. Introduction

After the discovery of the Higgs boson in 2012 by the ATLAS and CMS Collaborations [1, 2], the focus has shifted to measurements of its properties to test the predictions of the Standard Model (SM). A probe of fundamental interest is the coupling of the Higgs boson to the top quark, the heaviest elementary particle in the SM. A direct test of this coupling can only be performed through the production of a Higgs boson in association with a top-quark pair, $t\bar{t}H$. Still, this production process only contributes around 1% of the total Higgs boson production cross-section. It was observed based on the analysis of proton-proton collision data at $\sqrt{s} = 13$ TeV recorded with the ATLAS detector [3] at the Large Hadron Collider (LHC) using data corresponding to an integrated luminosity of up to $79.8\,\mathrm{fb}^{-1}$, and considering the Higgs boson decays into $b\bar{b}$, WW^*, $\tau^+\tau^-$, $\gamma\gamma$, and ZZ^*. In the following, the different analyses will be briefly summarised and their combination leading to the observation will be presented.

2. $H \to b\bar{b}$

The decay of a Higgs boson to a pair of bottom quarks has the largest branching fraction of about 58%. This decay mode is also sensitive to the Yukawa coupling of the b-quark. The analysis [4] targets events in which one or both top quarks decay semi-leptonically, producing an electron or a muon, and uses a dataset of $36.1\,\mathrm{fb}^{-1}$.

The main experimental challenge is to reconstruct and separate the signal from large backgrounds, mainly from $t\bar{t}$ + jets. To cope with this challenging background the events are categorised in nine signal (SRs) and ten control regions (CRs) either enriched in $t\bar{t}H$ or $t\bar{t}b$, $t\bar{t}c$, $t\bar{t}$ + light quarks. These regions are defined such that they are dominated by different flavour components of $t\bar{t}$ + jets, see Figure 1. In the single-lepton channel a dedicated lepton + jets boosted region is included. In the CRs the distribution of the scalar sum of the p_T of the jets, H_T, or the total yield is used to constrain the background in the fit. The SRs are fed into a two stage boosted decision tree (BDT). First, a reconstruction BDT is used to match jets to

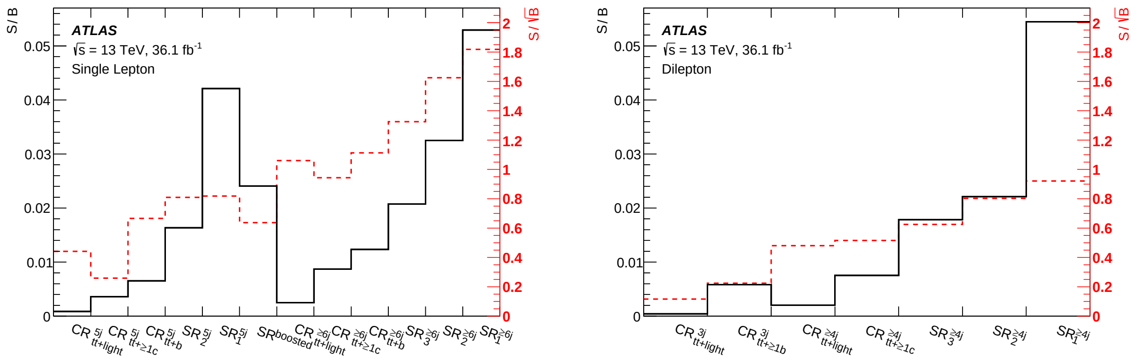

Figure 1. The ratio S/B (black solid line, referring to the vertical axis on the left) and $S/\sqrt{B}$ (red dashed line, referring to the vertical axis on the right) for each of the $H \to b\bar{b}$ analysis categories (left) in the single-lepton channel and (right) in the dilepton channel, where $S(B)$ is the number of selected signal (background) events predicted by simulation or through the data-driven estimates [4].

Higgs boson or top quark decays considering the large b-jet combinatorics. Also a likelihood discriminant or matrix element method are used for the reconstruction. The outputs of these three methods are given as input to the classification BDT. Here, the events are classified as more signal- or background-like, see Figure 2. To reduce uncertainties, a combined profile likelihood

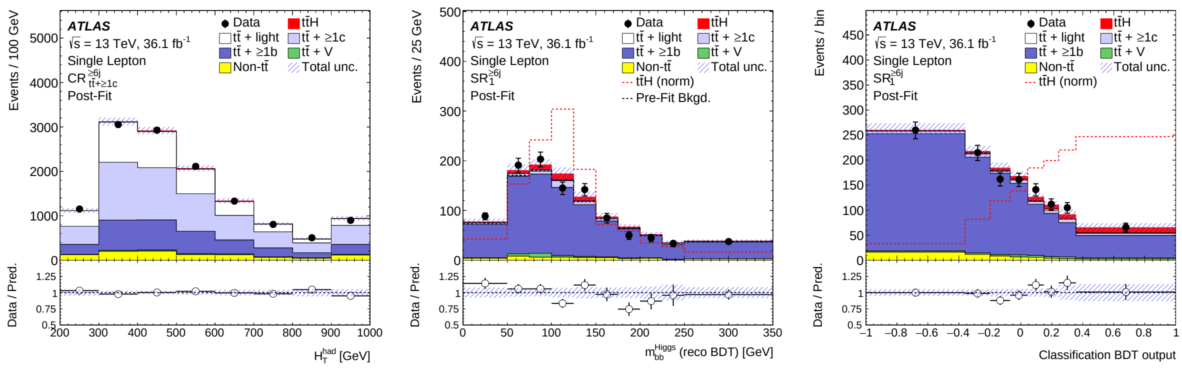

Figure 2. Distribution of H_{T} (left) and BDT outputs for the single lepton channel showing data (center) and background prediction for the $H \to b\bar{b}$ decay channel [4] (right).

fit to all 19 regions is performed. The uncertainty with the largest contribution is the $t\bar{t} + \geq 1b$ modelling. Overall, the analysis is dominated by systematic uncertainties but the statistical uncertainties of the Monte Carlo background modelling are also large. Considering this, a combined signal-strength of 0.84 is found, corresponding to an observed (expected) significance of 1.4 (1.6) standard deviations, see Figure 3.

3. $H \to$ multilepton

The multilepton analysis [5] considers the Higgs boson decays into WW^*, ZZ^*, $\tau^+\tau^-$ in a dataset of 36.1 fb^{-1}. The top-quark pair can decay into a single or dilepton final state. Seven different channels depending on the number of leptons and hadronic taus are considered and are split into

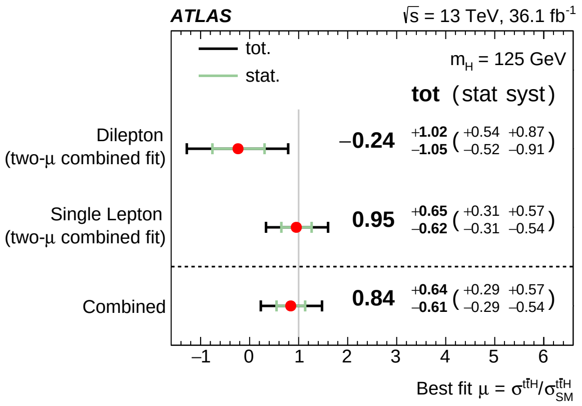

Figure 3. Signal-strength measurements in the individual channels and for the combination of the $H \to b\bar{b}$ decay channel. All the numbers are obtained from a simultaneous fit in the two channels, but the measurements in the two channels separately are obtained keeping the signal strengths uncorrelated, while all the nuisance parameters are kept correlated across channels [4].

eight SRs and four CRs, see Figure 4. Background contributions with prompt leptons originate

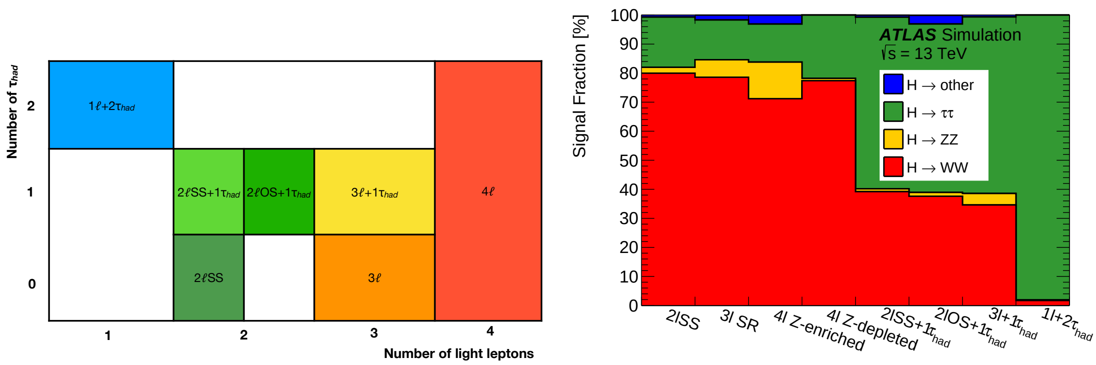

Figure 4. The channels of the $H \to$ multilepton analysis with corresponding Higgs boson decay modes [5]. Left: the channels used in the analysis. Right: the fraction of the expected $t\bar{t}H$ signal arising from different Higgs boson decay modes in each SR.

mainly from top production in association with a vector boson, $t\bar{t}W$, $t\bar{t}(Z/\gamma^*)$, and diboson production, VV. Data-driven methods are used to estimate non-prompt leptons and hadronic tau fakes. The modelling of this type of background is the greatest challenge of the analysis. To separate signal from background and to suppress backgrounds, a set of different BDTs is used. One dedicated BDT is used to reduce the misidentification of the electron charge, another BDT reduces the non-prompt electrons or muons. In the channels including taus, the fake contribution from hadronic tau fakes is a significant background and needs to be well modelled. Prompt electrons or muons are estimated from MC simulations. A maximum likelihood fit of the 12 categories is performed simultaneously to extract the $t\bar{t}H$ signal cross-section normalized to the prediction from the SM, see Figure 5. For five SRs a BDT shape is used as the final discriminant, whereas the total yield is used in regions with low statistics. The main systematic uncertainties are signal modelling and jet energy scale and resolution (JES/JER). Overall, the systematic and statistical uncertainties both account for $\sim 30\%$. A combined signal strength of 1.6 is found, see Figure 6. This corresponds to an observed (expected) significance of 4.1 (2.8) standard deviations and gives evidence for the $t\bar{t}H$ production.

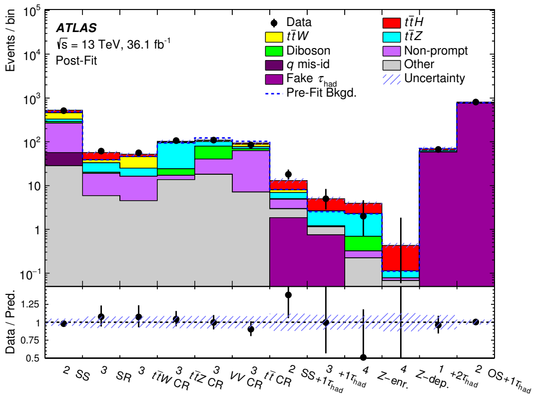

Figure 5. Observed number of events in data compared to the background and signal yields after the fit in the 12 fit regions for the $H \to$ multilepton decay channel [5].

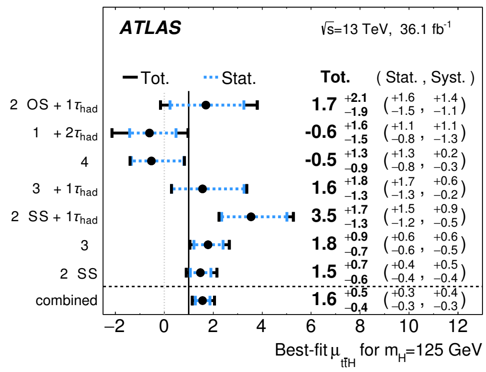

Figure 6. The observed best-fit values of the $t\bar{t}H$ signal strength μ and their uncertainties by final-state category and combined for the $H \to$ multilepton decay channel [5].

4. $H \to \gamma\gamma$

In the $H \to \gamma\gamma$ analysis [6] events with two isolated photon candidates are selected. The diphoton $m_{\gamma\gamma}$ invariant mass is chosen to be in the range $105\,\text{GeV} \le m_{\gamma\gamma} \le 160\,\text{GeV}$ and at least one b-tagged jet is required. Two signal regions are defined, a hadronic SR with at least two jets and zero isolated leptons, and a leptonic SR with at least one isolated lepton. A BDT is trained in each region with object-level variables, see Figure 7. The events are categorised

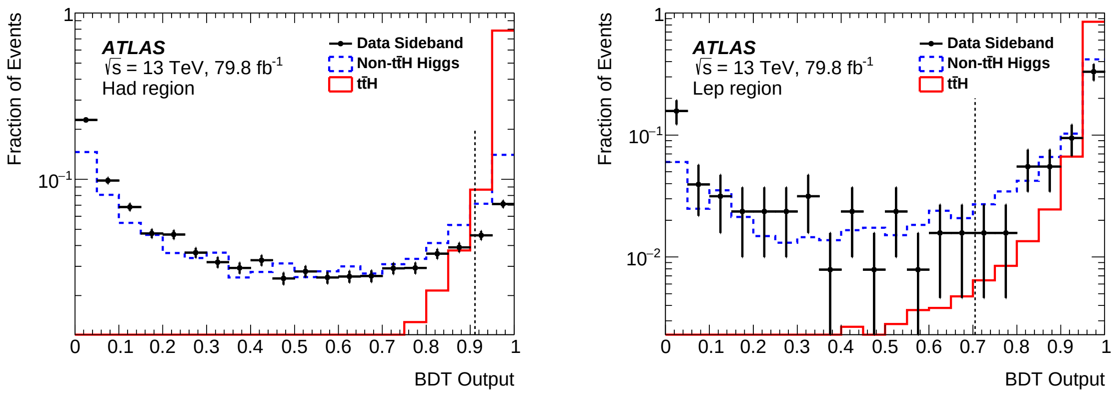

Figure 7. BDT output for the hadronic and leptonic signal regions for the $H \to \gamma\gamma$ decay channel. Events to the left of the vertical dashed line are rejected. The distributions are normalized to unity [6].

depending on the value of the BDT response in four (three) categories for the hadronic (leptonic) channel. This is done to optimize the sensitivity to the $t\bar{t}H$ signal. Figure 8 shows the weighted global fit of the diphoton mass.

The main systematic uncertainties are signal modelling, photon isolation and energy scale and resolution, and JES/JER. The event yields are presented in Figure 9, here a signal strength of 1.4 is assumed. With an observed (expected) significance is 4.1 (3.7) standard deviations also this analysis shows evidence for the $t\bar{t}H$ production.

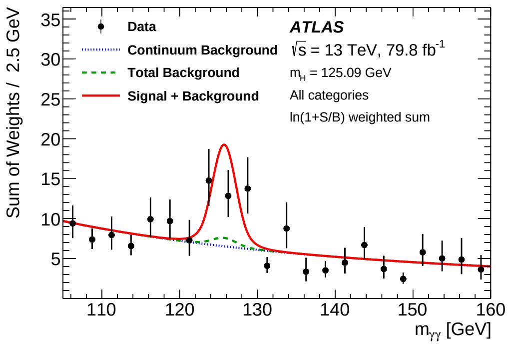

Figure 8. Weighted diphoton invariant mass spectrum in the $t\bar{t}H$-sensitive BDT bins for the $H \to \gamma\gamma$ decay channel [6].

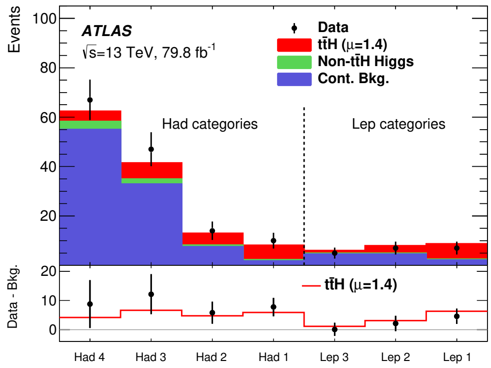

Figure 9. Number of events in the different regions for the $H \to \gamma\gamma$ decay channel [6].

5. $H \to ZZ^* \to 4\ell$

This channel was first considered for 13 TeV data [6] and uses a dataset of 79.8 fb^{-1}. Here, the Higgs boson decays in same flavour opposite sign pairs of four electrons, four muons, or two electrons and two muons. A Higgs candidate is considered within the range 115 GeV $\leq m_{4\ell} \leq$ 130 GeV, a region that is excluded from the $H \to$ multilepton analysis. Two signal regions enriched in $t\bar{t}H$ are selected by requiring at least one b-tagged jet. The hadronic SR requires in addition at least four jets and the leptonic SR requires in addition at least two jets and at least one lepton. In the hadronic region a BDT is employed to separate signal from background and the output discriminant is divided into two bins to maximize the expected significance, see Figure 10. No event is observed and as an upper limit $\mu < 1.8$ can be excluded

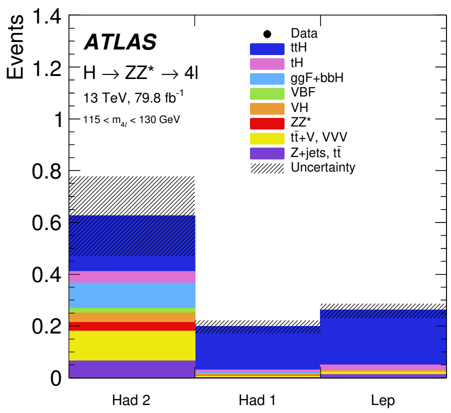

Figure 10. Number of expected events in the three bins, including systematic uncertainties. No events are observed in data. The bin with the higher values of the BDT discriminant and the leptonic region are expected to have a $t\bar{t}H$ signal purity of more than 80%. The other BDT bin is expected to have a $t\bar{t}H$ signal purity of about 35% [6].

at 68% C.L. The expected significance is 1.2 standard deviations.

6. Combination

Combining the $H \to b\bar{b}$, $H \to$ multilepton, $H \to \gamma\gamma$, and $H \to ZZ^* \to 4\ell$ analyses, the $t\bar{t}H$ production is observed. This is achieved with ATLAS Run-II data. When combining the 8 TeV and 13 TeV data, the expected significance is also larger than five standard deviations, see Table 1.

Table 1. Measured total $t\bar{t}H$ production cross-sections at 13 TeV, as well as observed (Obs.) and expected (Exp.) significances (sign.) relative to the background-only hypothesis [6].

Analysis	Integrated luminosity [fb^{-1}]	$t\bar{t}H$ cross section [fb]	Obs. sign.	Exp. sign.
$H \to \gamma\gamma$	79.8	$710\ ^{+210}_{-190}$ (stat.) $^{+120}_{-90}$ (syst.)	$4.1\ \sigma$	$3.7\ \sigma$
$H \to$ multilepton	36.1	790 ± 150 (stat.) $^{+150}_{-140}$ (syst.)	$4.1\ \sigma$	$2.8\ \sigma$
$H \to b\bar{b}$	36.1	$400\ ^{+150}_{-140}$ (stat.) $\pm$ 270 (syst.)	$1.4\ \sigma$	$1.6\ \sigma$
$H \to ZZ^* \to 4\ell$	79.8	<900 (68% CL)	$0\ \sigma$	$1.2\ \sigma$
Combined (13 TeV)	36.1−79.8	670 ± 90 (stat.) $^{+110}_{-100}$ (syst.)	$5.8\ \sigma$	$4.9\ \sigma$
Combined (7, 8, 13 TeV)	4.5, 20.3, 36.1−79.8	–	$6.3\ \sigma$	$5.1\ \sigma$

Figure 11 shows the ratios of the combined $t\bar{t}H$ production cross-section, as well as cross-sections measured in the individual analyses, to the SM prediction.

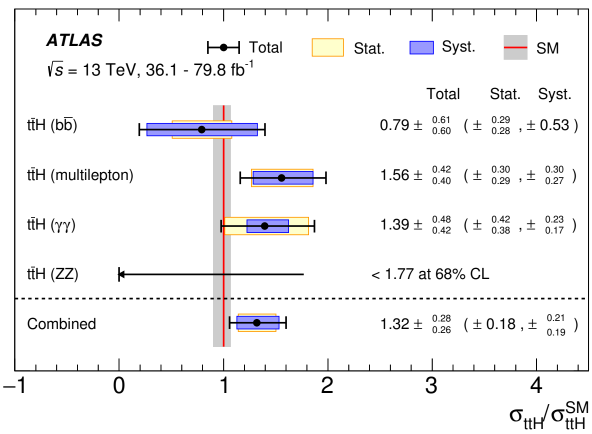

Figure 11. Combined $t\bar{t}H$ production cross-section, as well as cross-sections measured in the individual analyses, divided by the SM prediction [6].

7. Conclusion

In the combination, the production of the Higgs boson in association with a top-quark pair is observed with a significance of 6.3 standard deviations relative to the background-only hypothesis. The expected significance is 5.1 standard deviations.

Journal of Physics: Conference Series **1390** (2019) 012042 doi:10.1088/1742-6596/1390/1/012042

References

[1] ATLAS Collaboration 2012 *Phys. Let. B* **716** 1
[2] CMS Collaboration 2012 *Phys. Let. B* **716** 30
[3] ATLAS Collaboration 2008 *JINST* **3** S08003
[4] ATLAS Collaboration 2018 *Phys. Rev. D* **97** 072016
[5] ATLAS Collaboration 2018 *Phys. Rev. D* **97** 072003
[6] ATLAS Collaboration 2018 *Phys. Lett. B* **784** 173